geographies

MDPI

Article

Fire Severity Dynamics and Vegetation Recovery in Land Communal Areas Disturbed by *Pteridium aquilinum* in the Yucatan Peninsula

José Francisco López-Toledo [1,*], José Manuel Camacho-Sanabria [2], Juan Carlos Alcérreca-Huerta [3] and Pedro Antonio Macario-Mendoza [4]

[1] Instituto Tecnológico de la Zona Maya, Tecnológico Nacional de México, Ejido Juan Sarabia, Othón P. Blanco 77965, Quintana Roo, Mexico
[2] Secretaría de Ciencia, Humanidades, Tecnología e Innovación (SECIHTI), Universidad Autónoma del Estado de Quintana Roo, Campus Chetumal Bahía, Chetumal 77019, Quintana Roo, Mexico; jmanuelcs@live.com.mx
[3] Secretaría de Ciencia, Humanidades, Tecnología e Innovación (SECIHTI), El Colegio de la Frontera Sur (ECOSUR), Unidad Chetumal, Chetumal 77014, Quintana Roo, Mexico; jalcerrecah@ecosur.mx
[4] El Colegio de la Frontera Sur, Unidad Chetumal, Chetumal 77014, Quintana Roo, Mexico; pmacario@ecosur.mx
* Correspondence: jflopeztoledo@gmail.com

Abstract

Seasonal rainforests in the southern Yucatán Peninsula invaded by bracken fern (*Pteridium aquilinum*) are increasingly exposed to recurrent wildfires that may hinder native tree regeneration. Understanding fire severity dynamics and post-fire vegetation recovery is important for improving fire ecology knowledge and informing restoration strategies. This study evaluated wildfire severity and vegetation recovery in communal lands of the Yucatán Peninsula affected by *P. aquilinum*. Moderate-Resolution Imaging Spectroradiometer (MODIS) active-fire data were used to reconstruct fire history over a 22-year period, while Sentinel-2 imagery was employed to delineate burned areas following the 2020 and 2024 wildfire events. Fire severity was assessed using the differenced Normalized Burn Ratio (dNBR) with locally calibrated United States Geological Survey (USGS) thresholds, while supervised classification was applied to evaluate vegetation recovery one year after the 2020 wildfire. The study area exhibited a recurrent fire regime with an average fire-return interval of ~5 years and consistent fire-severity dynamics across both wildfire events. Areas dominated by *P. aquilinum* consistently experienced high fire severity and limited vegetation recovery, whereas areas with greater native tree coverage generally exhibited lower severity classes and more favorable recovery. These findings highlight the importance of controlling bracken fern dominance and promoting native tree recovery to enhance ecosystem resilience in tropical communal landscapes.

Keywords: fire ecology; fire recurrence; Mesoamerican rainforest; post-fire dynamics; remote sensing

Check for updates

Academic Editor: Marcos Francos

Received: 2 September 2026
Revised: 22 September 2026
Accepted: 24 September 2026
Published: 1 October 2026

Copyright: © 2026 by the authors. Licensee MDPI, Basel, Switzerland. This article is an open access article distributed under the terms and conditions of the Creative Commons Attribution (CC BY) license.

1. Introduction

Forest wildfires are a persistent threat to ecosystems worldwide, causing severe impacts on biodiversity, ecosystem structure, and ecological functioning [1–3]. Assessing fire-induced damage and understanding post-fire vegetation recovery over time are required for advancing fire ecology, informing restoration practices, and mitigating future wildfire risks [4–9]. Fire severity, commonly defined as the degree of ecosystem change

caused by fire [10,11], is a key metric for evaluating fire effects [12]. This assessment can be conducted using spectral indices derived from satellite imagery [13]. Landsat imagery with medium spatial resolution (30 m) has traditionally been used for this purpose [5]. Recently, Sentinel-2 Multispectral Instrument (MSI) imagery (20 m spatial resolution) has enabled finer-scale assessments of wildfire severity, improving the detection of spatial heterogeneity within burned areas [8,14].

The differenced Normalized Burn Ratio (dNBR) is among the most widely used spectral indices for severity analysis due to its strong correlation with field-based measures of fire damage [15,16]. This index integrates changes in vegetation biomass, canopy charring, moisture content, and soil disturbances caused by fire [17], providing a cost-effective approach for large-scale fire severity assessment using freely available Sentinel-2 imagery [13]. The dNBR derived from Sentinel-2 has been applied with thresholds established by the United States Geological Survey (USGS) in a variety of tropical ecosystems, including Brazilian shrublands [18], *Eucalyptus* plantations in Sri Lanka [19], and subtropical pine forests in India [20]. Because vegetation structure and fire behavior vary among ecosystems, several studies have refined these thresholds to improve fire severity assessments, such as in temperate forests of South Africa [17] and sclerophyll forests in Australia [21].

Although satellite-based fire severity assessments have become increasingly reliable, their application in tropical regions remains challenging. The analyses are often limited by the availability of cloud-free imagery, thus requiring specialized masking and image processing [19]. However, evaluating fire severity dynamics is relevant in tropical regions to assess degradation processes underway, particularly in areas with high wildfire recurrence, such as the southern Yucatan Peninsula. This region, part of the Mesoamerican rainforest and recognized as the second largest tropical rainforest in Latin America after the Amazon [22], has experienced significant disturbances in vegetation cover, which have altered the spatiotemporal patterns and severity of fires [23,24]. A primary factor of this degradation, particularly in communal land areas, is the invasion of fire-adapted bracken fern, *Pteridium aquilinum* (L.) Kuhn. This species produces large quantities of biomass through highly flammable dead fronds that facilitate fire ignition and spread [25,26]. Moreover, its ability to rapidly resprout from underground rhizomes after burning confers a competitive advantage over native species [27]. Consequently, recurrent wildfires favor the persistence of *P. aquilinum*, negatively impacting the regeneration of native tree species, which generally lack natural fire adaptations [7,27]. Despite ecological consequences of recurrent wildfires and bracken fern invasion documented in tropical ecosystems, their combined influence on long-term fire severity dynamics and post-fire vegetation recovery remains poorly understood, particularly for the southern Yucatán Peninsula.

Therefore, this study analyzes fire severity dynamics and vegetation response within communal lands of the seasonal rainforests of the southern Yucatán Peninsula, Mexico, invaded by *P. aquilinum*. For this purpose, historical fire occurrence was reconstructed using MODIS data over a 22-year period (2003–2024), while fire severity associated with the 2020 and 2024 wildfire events is described based on analyses of Sentinel-2 imagery and the dNBR index. Post-fire vegetation recovery was also analyzed through supervised image classification supported by field observations in communal tropical lands, offering information to support restoration and fire management strategies.

2. Materials and Methods

2.1. Study Area

This study focused on the communal land (ejido) of Rio Escondido, located in the southern Yucatán Peninsula, Mexico, within the Important Bird Area (IBA) 197, which is recognized for the conservation of bird populations and a broader biodiversity (Figure 1).

The study area is centered approximately at latitude 18°51′ N, and longitude 88°47′ W (i.e., 312,112 mE, 2,085,175 mN at UTM 16N). The area forms part of the Mesoamerican rainforest corridor and connects major natural protected areas in southeastern Mexico [28,29] (Figure 1).

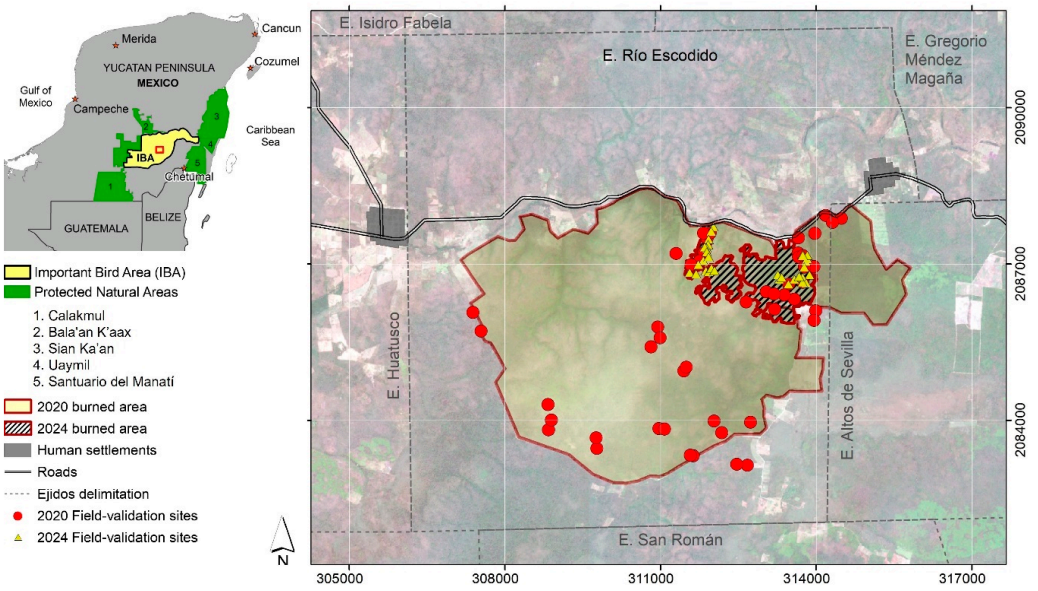


Figure 1. Location of the study area in the Yucatan Peninsula, Mexico, within the Important Bird Area (IBA) 197 [28], and surrounding Protected Natural Areas [29]. Burned areas in 2020 and 2024, as well as field-validation sites are shown, delimitation of communal land areas, known as 'ejidos' [30] and site infrastructure [31]. The stars represent the location of main cities un the Yucatan Peninsula.

The climate is classified as warm sub-humid (Aw1), with its landscape featured by karstic rock formations, rolling hills, local depressions, and elevations ranging from 50 to 180 m.a.s.l. Vegetation consists primarily of secondary tropical forests, including semi-evergreen forest and seasonally flooded lowland forests interspersed with agricultural land, pasture, and extensive areas invaded by *P. aquilinum* [32]. These invaded areas accumulate large amounts of fine, highly flammable biomass that increases fuel continuity and favors wildfire spread. In this regard, the area has experienced recurrent wildfires over the last two decades, including a large fire that occurred in March–April 2020, which affected ~2960 ha, followed by a subsequent event in April 2024, burning an additional 206 ha.

2.2. Wildfire Parameters, dNBR Index and Data Analysis

The frequency, recurrence and spatial extension of wildfires within the study area were analyzed for the period 2003–2024 using burned-area records derived from the MODIS sensor available through the Fire Information for Resource Management System (FIRMS; https://firms.modaps.eosdis.nasa.gov/). Following established procedures [33], fire frequency was defined as the total number of wildfire events recorded within the study area during the 2003–2024 period. Fire recurrence was calculated as the average interval (years) between consecutive fires occurring at the same location, whereas fire extent corresponded to the area affected by each wildfire event (ha).

Particularly for the 2020 and 2024 wildfires, burned perimeters were delineated and manually digitalized considering post-fire true-color and false-color infrared composites that allowed a clear distinction between burned and unburned areas. In this regard, Sentinel-2 L2A satellite imagery, which include radiometric and atmospheric correction, were acquired in true color (bands B_2, B_3 & B_4) and false-color infrared (bands B_3, B_4 & B_8) from the Copernicus platform (https://www.copernicus.eu/es; accessed on 7 June 2020,

24 February 2021 and 9 May 2024). For the 2020 wildfire, three pre-fire images (29 February, 5 March, and 25 March 2020) were combined to mask clouds and generate cloud-free composites (i.e., <10% cloud cover) as also conducted for two post-fire images (9 April and 19 May 2020). For the 2024 wildfire, a single pre-fire (29 March 2024) and post-fire image (3 May 2024) were used.

Additionally, fire severity recognizes that fire impacts alter vegetation structure and may lead to either recovery or further degradation over time [11,13,34]. Therefore, the fire severity was quantified using the dNBR spectral index, also derived from Sentinel-2 L2A satellite imagery using the composite images for the 2020 and 2024 wildfire events. The dNBR was computed through the difference between pre-fire and post-fire NBR values (Equation (1)), with NBR calculated according to Equation (2) using the near-infrared (NIR) band (B_8) and the shortwave infrared (SWIR) band (B_{12}):

$$dNBR = NBR_{pre\text{-}fire} - NBR_{post\text{-}fire} \quad (1)$$

$$NBR = (B_8 - B_{12})/(B_8 + B_{12}) \quad (2)$$

Fire severity classes were initially classified based on dNBR thresholds established by the USGS (https://un-spider.org/es/node/10959; accessed on 25 July 2020). The dNBR values ranged from −0.5 to 1.03, with higher-positive values indicative of greater fire severity, low values corresponding to unburned areas, and negative values suggest rapid post-fire vegetation recovery [10]. This initial dNBR assessment guided a field validation framework conducted in 2021 and 2024 that aimed to refine the delineation of fire severity classes. Using the dNBR values, a site-adjusted severity map was created.

Field assessments of the 2020 wildfire were conducted from June to August 2021, to examine vegetation recovery across severity classes. For the 2024 fire, fieldwork was carried out one month after the event to assess the immediate impacts of the fire. Fire severity results were finally compared across 2020 and 2024, with trends analyzed by overlaying severity maps.

2.3. Field Validation and Post-Fire Response

A stratified random sampling design was developed based on fire-severity classes derived from the dNBR index. Sampling sites were subsequently selected according to criteria of representativeness, accessibility, and field-survey safety. For the 2020 wildfire, 48 sampling plots of 400 m^2 each were established (Figure 1), distributed across the different severity classes: UB—unburned (n = 2), LS—low severity (n = 12), ML—moderate–low severity (n = 12 sites), MH—moderate–high severity (n = 18), and HS—high severity (n = 4). Furthermore, vegetation was classified into three structural strata according to its diameter at breast height (DBH): (i) trees (DBH $\geq$ 0.075 m), (ii) saplings (0.025 $\leq$ DBH < 0.075 m), and (iii) seedlings (DBH < 0.025 m). Trees were measured across the entire sampling plot of 400 m^2, while saplings were measured at 25 m^2 subplots, and seedlings within 1 m^2 quadrats.

Species identity and DBH were recorded for each individual, whereas basal area (BA) was calculated as in Equation (3), and subsequently standardized to m^2/ha according to the sampled area in hectare (0.04 ha for trees and 0.0025 ha for saplings). Similarly, plant density was standardized expressing the individuals per hectare (i.e., ind/ha). These parameters were used for the analysis of the vegetation structure across fire severity classes.

$$BA = (0.5 \cdot DBH)^2 \cdot \pi \quad (3)$$

Post-fire vegetation recovery following the 2020 wildfire was particularly evaluated using a Sentinel-2 L2A image from 3 February 2021 (<10% cloud cover). A supervised

land-cover classification was performed using 5510 training samples derived from field observations defining six land-cover classes: acahual, damaged acahual, young acahual, bracken fern, grassland, and bare soil. The resulting 2021 land-cover map was subsequently overlaid with the 2020 fire severity map to evaluate vegetation recovery across fire severity classes.

After the 2024 wildfire, 32 sampling plots were established (Figure 1), distributed among the same fire severity classes: UB (n = 1), LS (n = 9), ML (n = 5), MH (n = 11), and HS (n = 6). Assessment of fire severity in the field included estimates of percentage cover of trees, saplings, seedlings, litter, and bare soil, together with measurements of stem and crown scorch heights (m) and visual damage appraisal (%), following [35]. Slope and soil stoniness were recorded as site variables and potential indicators of fire history. In addition, regression analyses were performed to evaluate the relationships between dNBR values and stem scorch height, litter cover, and visual damage.

Finally, oblique aerial imagery in 2024 was acquired at four sites using a DJI Mini 2 drone (Shenzhen, China). Flights were conducted at an altitude of 120 m with a 50° downward camera angle as complementary visual information to assess vegetation structure and to verify the spatial consistency of the dNBR-derived fire severity classification. Drone images were collected in eight viewing directions (N, NE, E, SE, S, SW, W, and NW). These images, complemented by field observations collected during the establishment of the sampling sites, enabled the characterization of spatial heterogeneity, the identification of transition zones between severity categories, and the differentiation of fire-affected areas from those affected by other disturbances.

3. Results

3.1. Fire History and Recurrence

MODIS fire records documented five fire events during the 22-year study period (2003–2024), corresponding to a mean interval of 5.25 years between recorded fires. Fire recurrence became more regular after 2011, suggesting a recurring fire pattern within the study area. The wildfires in 2003 and 2011 occurred toward the end of the dry season (May and June) (Figure 2a,b), whereas the three most recent fires (2015, 2020 and 2024) occurred earlier in the season, during March and April (Figure 2c–e). Particularly for the wildfire events in 2015 and 2020, burned areas occurred in two consecutive months, first developing in the northern portion of the study area and mainly further extending to the south.

The largest wildfire extent recorded in the study area occurred in 2020, covering ~2660 ha based on estimates from MODIS data. For this event, the MODIS-derived burned area accounted for approximately 90% of the area delineated considering Sentinel-2 imagery (2960 ha). Using the MODIS-derived burned area in 2020 as the reference, the fires in 2011 and 2015 were the most extensive, affecting nearly 81.6% and 64.7% of the area, respectively. In contrast, the smallest wildfire events occurred in 2003 and 2024, affecting 34.1% (~907 ha) and 12.3% (~327 ha) of the 2020 reference area, respectively (Figure 2). In comparison with Sentinel-2 imagery, the burned area delineated for the 2024 event resulted in 206.1 ha, equivalent to 6.96% of the Sentinel-2 2020 burned area (2960 ha).

Notably, the wildfires in 2003, 2015, and 2020 were confined to the ejido Rio Escondido and showed a similar spatial development. In contrast, the 2011 and 2024 wildfires extended beyond the 2020 fire boundaries, affecting adjacent communal lands, including the ejido Altos de Sevilla. It is important to clarify that the abovementioned percentages of burned areas were calculated exclusively within the 2020 reference, so that areas burned by the 2011 and 2024 fires that extended beyond this boundary were not considered. Consequently, the total burned areas for these two years may be larger than indicated by the reported percentages. These values should therefore be interpreted as the proportion of

the 2020 reference area affected by fire, rather than as estimates of the total burned area for each year.

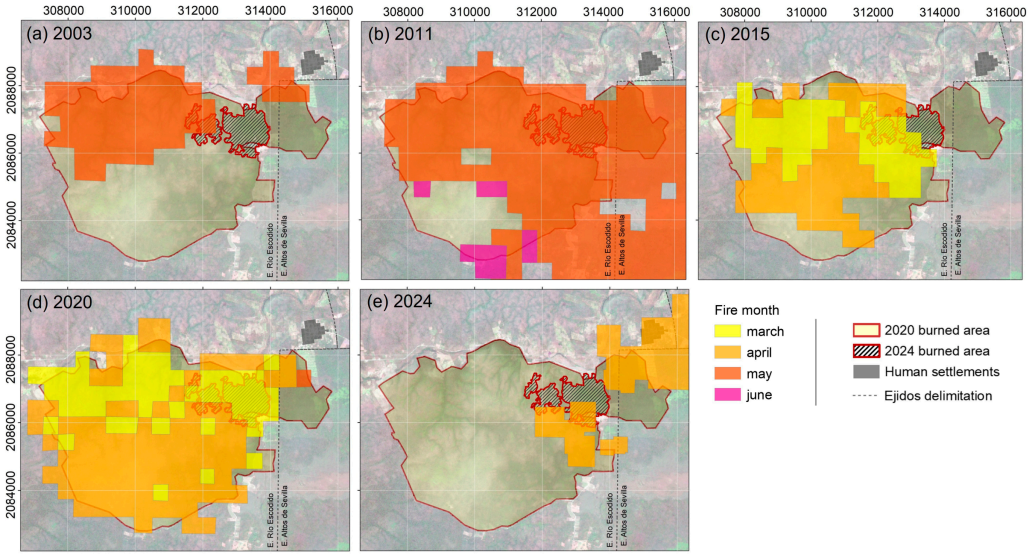


Figure 2. Monthly fire history in the study area in 2003 (**a**), 2011 (**b**), 2015 (**c**), 2020 (**d**) and 2024 (**e**). Burned areas detected by the MODIS sensor (FIRMS: https://firms.modaps.eosdis.nasa.gov/) are represented. Delimitation of 2020 and 2024 burned areas delineated with higher-resolution Sentinel-2 imagery is overlaid for comparison.

3.2. Fire Severity Classification and Field Validation

Field validation of the 2024 fire severity map showed that areas initially classified as low severity (LS; dNBR = 0.10–0.27), according to the standard USGS thresholds, presented no evidence of fire damage and were therefore reclassified as unburned (UB). Field surveys conducted on May 3rd, 2024, further indicated that much of the vegetation was undergoing seasonal dry-season defoliation, which likely increased dNBR values pointing them into the LS class. Based on the observations and the resulting dNBR values, four severity classes were considered: UB—unburned (dNBR = 0.00–0.27), ML—moderate–low (dNBR: 0.27–0.44), MH—moderate–high (dNBR: 0.44–0.66), and HS—high (dNBR: >0.66).

Correlations between dNBR values and three field-based indicators of fire severity were assessed for the 2024 fire, including (a) scorch stem height (SH), (b) litter cover (LC), and (c) overall damage appraisal (DA) (Figure 3). The relationship between the SH and dNBR was described by an exponential model (Equation (4)), indicating a rapid increase in stem scorch height with increasing fire severity. Also, LC and DA were fitted by hyperbolic tangent functions (Equations (5) and (6)), producing sigmoidal response curves constrained at dNBR = 0 (i.e., LC = 100% and DA = 0%) and dNBR at higher values (i.e., LC = 0% and DA = 100%).

$$SH = 0.064 \cdot e^{5.35\ dNBR} \quad (4)$$

$$LC = [1 - \tanh(10.9 \cdot dNBR^{2.5})] \cdot 100 \quad (5)$$

$$DA = [\tanh(216.4 \cdot dNBR^{5.0})] \cdot 100 \quad (6)$$

The variables SH and DA described a positive correlation with dNBR-values, with coefficients of determination (R^2) of 0.65 and 0.92, respectively (Figure 3a,c). In contrast, LC showed an inverse relationship with dNBR, with the fitted model describing a coefficient of determination $R^2 = 0.78$ (Figure 3b).

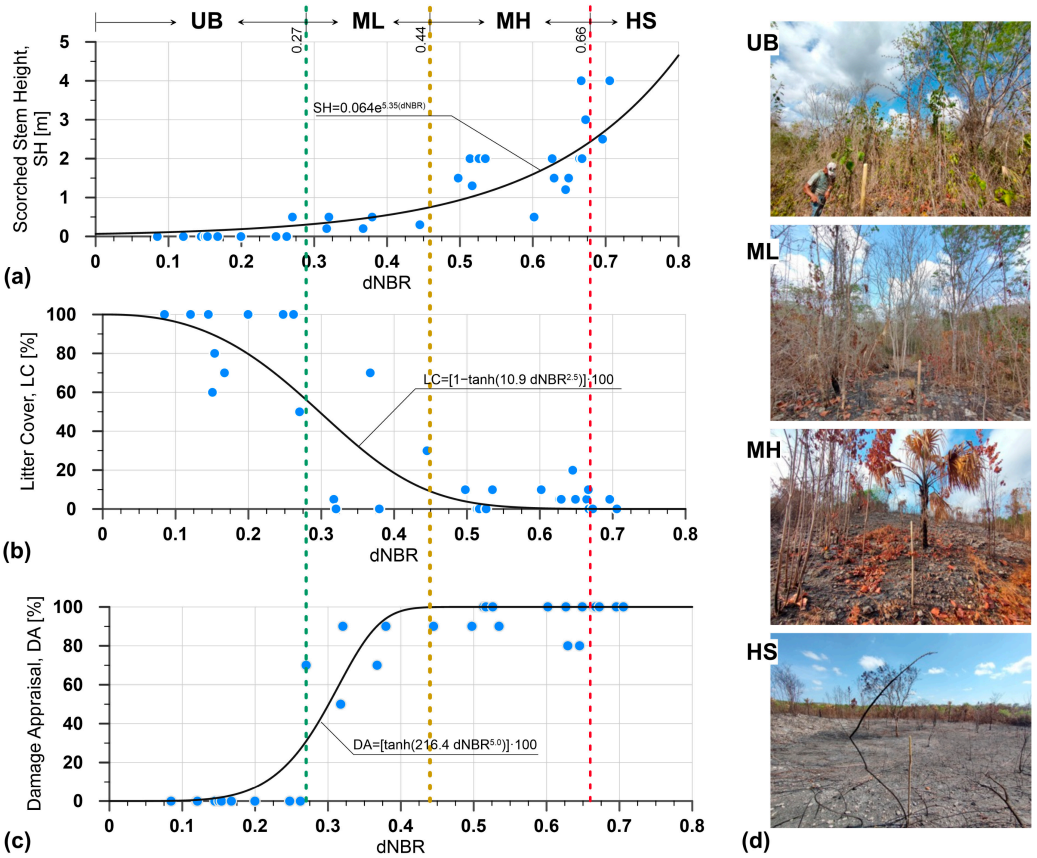


Figure 3. Damage relates [(**a**) scorch stem height (SH), (**b**) litter cover (LC) and (**c**) damage appraisal (DA)] of fire 2024 with dNBR values and visual appearance in the field of fire severity classes (**d**).

Litter cover (LC) declined markedly along the fire severity gradient, decreasing from 100.0 to 60.9% in UB areas to 11.5% under ML conditions, with little or no litter remaining in MH and HS conditions. According to Equation (5), the most pronounced reduction occurred at a dNBR value of approximately 0.31, where nearly half of the original litter cover had been consumed (Figure 3b). In contrast, DA increased from 0% in UB areas to 59.0% at a dNBR value of 0.316, corresponding to ML conditions. Above this threshold, DA continued to increase more gradually, approaching maximum values in MH and HS areas (Figure 3c).

The UB areas showed no evidence of recent fires and were characterized by a taller tree cover, sapling and seedling strata, particularly in regions exposed to sunlight. Abundant organic matter was also observed covering the soil surface (Figure 3d-UB, Table 1). Under moderate–low severity (ML), the seedling layer was almost entirely consumed, while less than 50% of the litter layer was burned (<50%). In these areas, saplings and mature trees showed a reduction in live tree cover relative to UB conditions, although damage was less severe than in the MH and HS classes (Figure 3d-ML, Table 1).

At the MH-severity class, the fire impact was more pronounced among the tree and sapling strata. Although stems were not completely consumed, high mortality was observed, resulting in substantial leaf litter accumulation and scorch marks on stems, reaching up to 2.0 m in height (Figure 3d-MH, Table 1). In high-severity (HS) areas, litter cover was almost absent (<10%) and soil was completely bare (>90%). Isolated individuals of *Sabal yapa* persisted from previous fire events and remained in the landscape. However, the post-fire vegetation was dominated by fire-tolerant species, particularly *P. aquilinum* and *S. yapa*, which largely displaced the surviving native vegetation (Figure 3d-HS, Table 1).

Table 1. Traits observed in the field at the different severity classes for the 2024 fire event in the study area.

Traits		Severity Class			
		UB	**ML**	**MH**	**HS**
Tree cover	[%]	>70	>70	<70	<30
Live tree cover	[%]	>70	10 to 30	<10	0
Sapling cover	[%]	>30	10 to 30	<50	0
Seedling cover	[%]	<40	0	0	0
Litter cover	[%]	>70	<50	<20	<10
Bare soil	[%]	<20	50 to 100	70 to 100	>90
Scorch stem height	[m]	0	0.2 to 0.5	0.5 to 2.0	2.0 to 4.0
Scorch crown height	[m]	0	2.0 to 4.0	2.0 to 6.0	3.0 to 6.0
Damage appraisal	[%]	0	70 to 90	80 to 100	100

Note: Tree cover includes standing dead trees, while live tree cover only reflects surviving trees.

UAV (Unmanned Aerial Vehicle) imagery supported the spatial field validation of the dNBR-derived fire severity classes and provided additional evidence of the spatial gradient pattern transitioning from unburned (UB) to high severity (HS) conditions (i.e., UB → ML → MH → HS) (Figure 4). This gradient was associated with distinct vegetation structures and landscape characteristics across the fire severity classes.

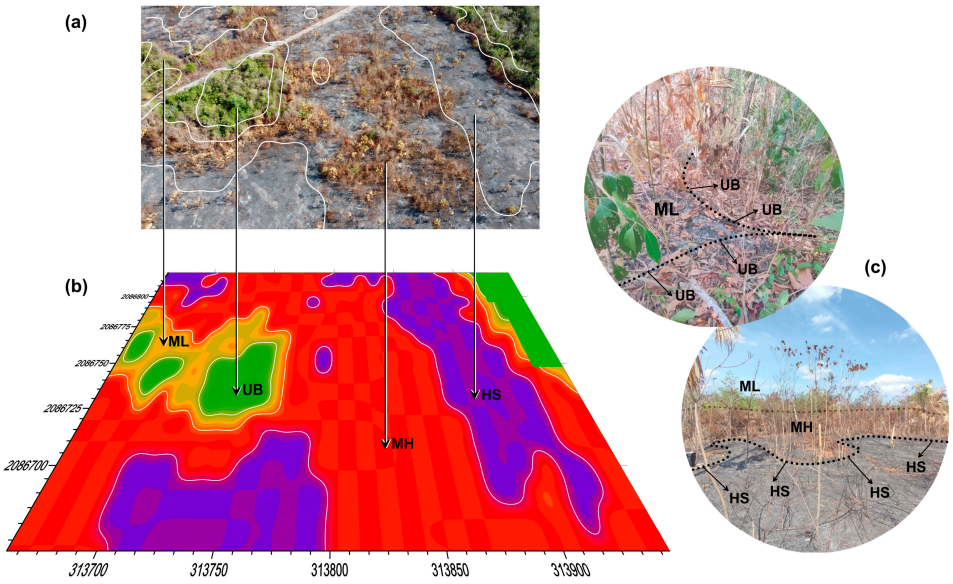


Figure 4. Fieldwork validation for the severity classes after 2024 fire: (**a**) aerial oblique view from UAV at an altitude of 120 m and camera tilted 50° downward from the horizon; (**b**) corresponding oblique view of the severity map aligned with the aerial image; (**c**) field view illustrating the transitions between distinct severity class.

The UB severity class primarily occurred in areas with dense tree cover and low-lying terrain depressions featured by high soil moisture or standing water, which inhibited fire spread (Figure 4a). ML severity was mainly found along forest edges and ecotones (i.e., transition zones between open areas and tree-dominated vegetation). In these locations, fire effects were limited, with relatively minor damage to trees and saplings (Figure 4c).

MH severity areas were characterized by lower tree density but retained sapling and seedling strata. Fire effects were substantially greater, resulting in high mortality of almost all the vegetation, although dead stems were not completely consumed. Finally, the HS severity occurred in areas dominated by herbaceous vegetation, particularly

P. aquilinum, where combustible biomass was almost completely consumed. An exception was provided by *S. yapa* palms, which persisted within the burned landscape, consistent with their apparent resilience to recurrent fire (Figure 4c).

3.3. Fire Severity Dynamics

The analysis using a field validation of dNBR classes delineated a total mapped fire extent of ~2960.0 ha in 2020, distributed among four fire severity classes. MH-severity occupied the largest proportion of the burned area, covering ~1713.8 ha (57.9%), followed by ML-severity, which covered ~768.1 ha (26.0%). UB areas within the fire perimeter accounted for ~317.6 ha (10.8%), whereas HS-severity areas represented ~160.3 ha (5.4%) (Figure 5a).

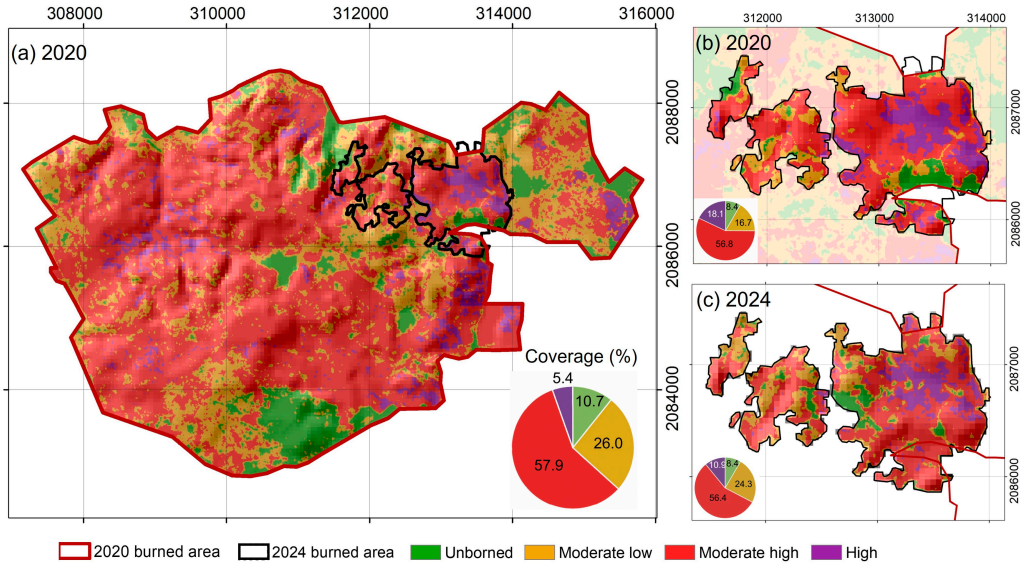


Figure 5. Severity classes and cover percentage, derived from adjusted dNBR thresholds of the 2020 (**a**,**b**) and 2024 (**c**) fires in the study area. Detail of the 2020 severity classes within the recurrent burned area in 2024 is shown in (**b**) for comparison purposes.

The 2024 wildfire event affected ~206.1 ha and exhibited a fire severity distribution comparable to that observed in 2020. MH severity again represented the largest proportion, covering 116.3 ha (56.4%), followed by ML (50.0 ha; 24.3%), HS (22.5 ha; 10.9%), and UB (17.3 ha; 8.4%) (Figure 5c).

An overlay comparison of the 2020 and 2024 severity classes within the common polygon extent (Figure 5b,c) showed a 7.1% decrease in the proportion of HS almost compensating a 7.6% increase in ML, whereas the proportions of UB and MH remained relatively stable between the two wildfire events. Overall, the similar distribution of severity classes suggest that the fire severity patterns might vary minimally between consecutive fire events and indicate a broadly consistent and recurrent spatial structure of fire severity across the study area.

3.4. Post-Fire Vegetation Response

One year after the 2020 wildfire, bare ground and five vegetated land cover types were observed within the fire-affected areas: acahual, damaged acahual, young acahual (in transition), bracken fern (*P. aquilinum*), and grassland.

The acahual represents a secondary-growth vegetation associated with semievergreen tropical forest and seasonal lowland flooded forest in Mexico. From field-observations, a seasonal lowland flooded forest of this vegetation dominated where clay-rich sediments accumulate and seasonal flooding occurred during the rainy season. On the other hand,

semievergreen tropical forest was noticed at relatively elevated and better-drained areas. Among the vegetation cover types, acahual exhibited the highest density of trees (DBH $\geq$ 7.5 cm) and saplings (DBH $\geq$ 2.5 and <7.5 cm), as well as the largest basal area (BA). Dominant tree species included *Vitex gaumeri* Greenm., *Bursera simaruba* (L.) Sarg., and *Piscidia piscipula* (L.) Sarg., which occurred under both micro-relief conditions (Table 2).

Table 2. Vegetation structure, including density (D) (ind./ha), basal area (BA) (m2/ha), and dominant species (Sp), across the land covers identified in 2021 within the 2020 fire-affected area. Land covers include SG (secondary-growth vegetation), SE (semievergreen tropical forest), SL (seasonal lowland flooded forest), and H (herbaceous vegetation).

Land Cover	Vegetation Type	Trees			Saplings			Seedlings
		D	BA	Sp	D	BA	Sp	Sp
Acahual	SG/SE & SL	400 to 1000	5 to 12	Vg	1000 to 8000	2 to 7	Bs	Tr
Damaged Acahual	SG/SE & SL	100 to 400	<7	Bs	400 to 1200	5 to 15	Cs	Ns
Young Acahual	SG/SE & SL	<500	<10	Sy	400 to 6000	<10	Cs	Pa
Bracken fern	H	<100	<3	Sy	<1000	<1	Bs	Pa
Grassland	H	<20	<3	Sy	<1000	<2	Pp	Ub
Bare ground	None	0	0	0	0	0	-	-

Bs: *Bursera simaruba* (L.) Sarg., Cs: *Coccoloba spicata* Lundell, Ns: *Nectandra salicifolia* (H.B. & K.) Nees, Pa: *Pteridium aquilinum* (L.) Kuhn, Pp: *Piscidia piscipula* (L.) Sarg, Sy: *Sabal yapa* C. Wright ex Becc., Tr: *Thrinax radiata* Lood. ex J.A. & J.H. Schutt., Ub: *Urochloa brizantha* (Hochst. ex A. Rich.) R. D. Webster, Vg: *Vitex gaumeri* Greenm.

Acahual covered 13.7% of the analyzed area and was primarily distributed in areas of relatively low stoniness with slopes <15%. Most of these acahual areas were associated with the ML-severity class, consistent with relatively rapid post-fire vegetation recovery (Figure 6, Table 3). However, damaged acahual retained visible evidence of fire effects from the 2020 fire. This cover type showed 20–50% tree mortality and a notable reduction in the density of live trees (Table 2). Species such as *Bursera simaruba* (L.), *Lysiloma latisiliquum* (L.) *Benth.*, and *Metopium brownei (Jacq.) Urban* were commonly observed in this condition. Although their relationship with severity was similar to that of undamaged acahual, fire-related damage remained detectable in Sentinel-2 imagery even one year after the 2020 fire event (Figure 6).

Open areas with low tree density (<100 individuals/ha), were dominated by *S. yapa* palms and almost entirely covered by *P. aquilinum* often featuring the bracken fern land cover (Table 2). Bracken fern was the second most extensive cover type, occupying 19.6% of the study area. It was predominantly associated with MH severity and showed a strong association with HS areas (Figure 6, Table 3).

The transitional stage between bracken fern and acahual was represented by young acahual cover type, possibly related to the local rainforest recovery after fire events and bracken fern invasion. Although this stage showed a low density of trees, it showed a higher number of saplings and seedlings, mainly of species such as *Coccoloba spicata* Lundell, *Trema micrantha* (L.) Blume, and *Piscidia piscipula* (L.) Sarg., which primarily resprouted after a fire event. In this cover type, the dominance of *S. yapa* palms and the presence of *P. aquilinum* were indicative of its association with areas previously affected by fire (Table 2). Young acahual was the most extensive cover type, occupying 48.4% of the study area. It was primarily associated with MH severity and occurred on slopes ranging from 10 to 35%, where soil stoniness commonly varied between 50% and 90% (Figure 6; Table 3).

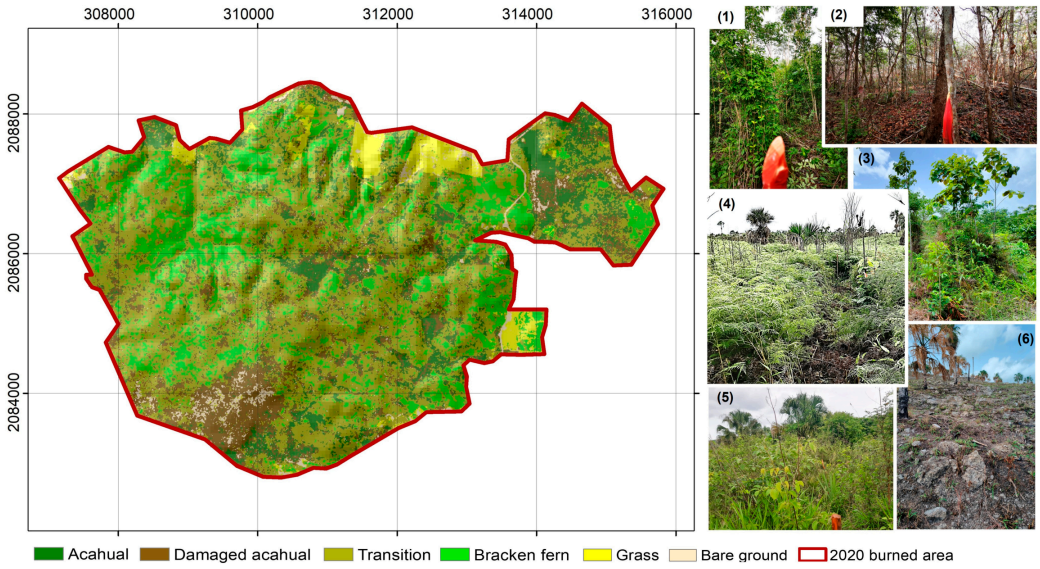


Figure 6. Land cover types observed in 3 February 2021, following the 2020 fire event. Visual recognition of land covers is also shown for: (**1**) acahual, (**2**) damaged acahual, (**3**) young acahual or transition from bracken fern to acahual, (**4**) bracken fern, (**5**) grass, and (**6**) bare ground.

Table 3. Areas in hectares and percentages (inside parenthesis) of the post-fire land covers identified on February 3rd, 2021, in relation to the severity classes of the 2020 fire event.

Severity Class		Land Covers *						
		A	**DA**	**YA**	**BF**	**G**	**BG**	**Total**
UB	ha	92.14	44.13	114.77	14.46	34.89	17.21	317.6
	(%)	(3.11)	(1.49)	(3.88)	(0.49)	(1.19)	(0.59)	(10.75)
ML	ha	197.3	175.63	273.02	42.5	47.72	31.91	768.08
	(%)	(6.67)	(5.93)	(9.22)	(1.44)	(1.61)	(1.08)	(25.95)
MH	ha	115.28	114.67	1023.92	387.15	42.24	30.68	1713.94
	(%)	(3.89)	(3.87)	(34.59)	(13.08)	(1.43)	(1.04)	(57.9)
HS	ha	0.61	0.27	20.23	134.9	4.24	0.04	160.29
	(%)	(0.02)	(0.01)	(0.68)	(4.56)	(0.14)	(0.00)	(5.41)
Total	ha	405.33	334.7	1431.94	579.01	129.09	79.84	2959.91
	(%)	(13.69)	(11.3)	(48.37)	(19.57)	(4.37)	(2.71)	(100.00)

* A—acahual, DA—damaged acahual, YA—young acahual, BF—bracken fern, G—grassland, BG—bare ground.

Grassland was observed in areas used for cattle grazing, with dominance of *Urochloa brizantha* (Hochst. ex A. Rich.) R. D. Webster. Field observations indicated that these pastures were typically burned for vegetation renewal and removal of competing native vegetation (Table 2). This cover type presented no apparent relationship with the HS-class (Table 3). Additionally, areas with little or no vegetation cover were also identified as bare ground and were mainly related to sites affected by cattle grazing or recent burning as part of cultural practices for agricultural land preparation (Table 2). These areas were found mainly associated with ML- and MH-severities classes (Figure 6, Table 3).

4. Discussion

Seasonal rainforests are highly sensitive to fire, which severely alter their vegetation structure, composition, and biodiversity [36,37]. This vulnerability is exacerbated when

recurrent fire interacts with disturbance-associated species such as *P. aquilinum*, creating a reinforcing disturbance regime [6]. Repeated burning can reduce opportunities for native vegetation recovery and favor species capable of rapidly colonizing or resprouting after disturbance. This may drive the system towards alternative stable states that usually require specialized restoration interventions [38].

The approximately five-year mean interval between recorded fires in areas affected by *P. aquilinum* is broadly consistent with recurrence patterns reported by [39] in Indonesian rainforests. These results contrast with [27], who proposed a two- to three-year recurrence interval under environmental conditions comparable to those examined in this study. These differences and the present findings suggest that fire recurrence may vary according to local fuel accumulation, vegetation structure, climatic conditions, and land-use practices. Although the temporal record analyzed here does not by itself demonstrate a statistically defined fire cycle, the repeated occurrence of fire at relatively short intervals, together with the persistence of *P. aquilinum*-dominated vegetation, is consistent with the alternative stable states' framework proposed for fire-prone landscapes invaded or dominated by this species [38].

The integration of MODIS and Sentinel-2 data provided complementary information on fire-severity dynamics across different spatial and temporal scales. MODIS observations enabled the reconstruction of fire occurrence over the 2003–2024 period, whereas Sentinel-2 imagery provided a finer-scale spatial characterization of individual fire events and their severity. The incorporation of UAV imagery and field observations further strengthened the spatial validation of the dNBR fire-severity classification and improved the delineation of burned areas.

This multi-scale approach showed that recurrent fires were spatially associated with distinct vegetation conditions, particularly areas characterized by dense *P. aquilinum* cover, whereas areas with greater tree cover generally exhibited lower fire severity or remained unburned. These patterns suggest that recurrent fires may be linked to the persistence or expansion of particular vegetation conditions rather than representing isolated, independent wildfire events. This finding highlights the value of integrating satellite observations with field- and UAV-based data to characterize fire severity and its spatial heterogeneity in tropical landscapes. Nevertheless, comparisons of fire extents derived from MODIS and Sentinel-2 should be interpreted with caution, as differences in spatial resolution can influence burned-area estimates. In particular, the coarser spatial resolution of MODIS might affect burned area estimates when fire boundaries are heterogeneous or fragmented, whereas finer-resolution Sentinel-2 imagery can more effectively delineate the spatial extent of smaller fire events, as illustrated by the 2024 event.

The dNBR proved its functionality in distinguishing severity classes even in heterogeneous tropical ecosystems [17,21,33]. However, the dNBR-based analysis demonstrated the importance of accounting for vegetation phenology when applying generalized fire-severity thresholds. In this study, areas classified as low severity using the standard USGS thresholds showed no field evidence of recent burning and were instead associated with vegetation undergoing seasonal dry-season defoliation. This finding indicates that phenological changes can influence analyses of post-fire spectral responses, potentially leading to an overestimation of fire severity when generalized thresholds are applied without local calibration. This aligns with [39] and the recommendation to adjust dNBR thresholds for each specific region and land cover type, while [21] suggested to incorporate additional spectral indices in such cases. This result is particularly relevant for seasonal tropical forests, where pronounced changes in vegetation phenology during the dry season might overlap spectrally with fire-related responses. Moreover, it offers valuable insights into

post-fire landscape dynamics and the differential impacts of fire across a severity gradient, particularly in local disturbed seasonal rainforests.

The spatial distribution of severity classes further revealed a strong association between fire effects and vegetation structure. Areas with denser tree cover generally exhibited lower severity or remained unburned, whereas areas dominated by herbaceous vegetation experienced higher severity (Table 4). Notably, areas covered by dense *P. aquilinum* biomass associated with HS class. A similar relationship between fine, continuous herbaceous fuels and greater combustion completeness has been reported in Mediterranean ecosystems [40].

Table 4. Summary of damage, fire behavior, and response/characteristics of vegetation at different fire severity classes based on the findings of field-validation work and analysis of satellite imagery within the disturbed tropical rainforest in the study area.

Class	Pre-Fire Fuel Type	Coverage 1-Year After Fire	Characteristics of Affected Areas	Fire Behavior	Damages
UB	High density tree vegetation	Acahual, young acahual, grass	Humid lowlands, low fuel load.	No flammable conditions.	No damage.
ML	Fragmented tree vegetation	Acahual, damaged acahual, young acahual	Perimeters of forest stands, ecotones, fragmented forest, moderate fuel load.	The fire burned with low intensity due to factors that slowed it down.	Partial consumption of organic matter, no presence seedlings, scorched stems height <50 cm.
MH	Shrub and herbaceous vegetation	Young acahual, bracken fern	Transition between bracken fern and young acahual, high fuel load (litter and fern fronds).	The fire burn with high intensity, killed saplings and seedlings but did not consume their stems.	Partial mortality of trees, total mortality of saplings and seedlings, scorched stems height up to two meters.
HS	Herbaceous vegetation	Bracken fern	High fuel load (fern fronds).	The fire consumed everything except palms *Sabal yapa*.	Total calcination except for adult palms, bare ground.

The post-fire vegetation patterns provide further evidence of potential feedback between recurrent fire and vegetation composition. Repeated exposure to high-severity fires might increase soil exposure, reduce nutrient availability, and favor the persistence of opportunistic species such as *P. aquilinum*, thereby reinforcing degradation processes already described in tropical ecosystems [18,27]. Conversely, areas of lower fire severity supported greater tree and sapling densities and showed more advanced development of secondary vegetation as also described by [40]. These areas were primarily located in areas with moderate tree cover, such as forest margins (ecotones), fragmented forest patches, and cultivated land boundaries (Table 4). Moreover, ML severity appeared to represent an intermediate condition between unburned and moderate–high severity areas. In this context, ref. [21] highlights the role of plant community composition in determining how fire intensity translates into severity.

The similarity in fire severity patterns observed between the 2020 and 2024 wildfire events suggests the persistence of a fire–vegetation feedback mechanism. Areas dominated by *P. aquilinum* consistently exhibited higher fire severity and limited vegetation recovery. These patterns indicate that vegetation composition may contribute to the persistence

of recurrent fire dynamics in the study area [27,38]. Recurrent burning might favor the persistence and expansion of fire-tolerant vegetation, while changes in fuel continuity and structure could, in turn, maintain conditions conducive to subsequent fires. Such feedback could reinforce fire-prone conditions by promoting fuel accumulation, limiting forest recovery, and increasing the likelihood of future fire events.

Field observations indicated a pronounced transition between unburned and moderate–low severity conditions, featured by a rapid reduction in litter cover and an increase in visual damage. This suggests that relatively small increases in fire severity could promote rapid changes and ecological impacts, particularly in areas with continuous and highly flammable fine fuels such as *P. aquilinum*. This could also promote rapid shifts in fire behavior and post-fire vegetation conditions as described by [39].

As described in Table 4, supervised classification of Sentinel-2 imagery and field observations allowed to relate severity to the resulting vegetation covers, providing insights into the post-fire response in areas disturbed by *P. aquilinum*. The observed response is featured by a strong relation between severity classes, the post-fire vegetation type, and the dominance trend of vegetation capable of resprouting after fire events [39]. The recurrence of HS conditions in areas dominated by *P. aquilinum*, together with limited development of native woody vegetation, leads to a trajectory toward persistent herbaceous dominance and forest degradation. Such conditions are consistent with processes of potential savannisation and reduced native species diversity described for recurrently burned tropical landscapes [27,37,41,42] (Table 4). Also, the absence of a tree canopy over herbaceous vegetation accelerates fuel desiccation [36], and strengthens the possibilities of increasing the recurrence of tropical wildfires.

Human activities can either reduce or increase fire risk depending on their intensity, timing, and spatial configuration. Practices such as the establishment of firebreaks, grazing to reduce fine-fuel accumulation, and vegetation clearing associated with traditional agriculture can modify fuel continuity and, when appropriately planned and implemented, contribute to fire prevention.

The findings of this study suggest that fire-resilient landscape configurations could be promoted by maintaining spatial discontinuities in combustible vegetation and conserving areas with greater moisture retention, particularly those characterized by high tree cover and low-lying terrain. Such landscape features may interrupt fuel continuity and reduce fuel desiccation, thereby limiting the potential for high-severity fire, consistent with the mechanisms described by [43].

The spatial characterization of vegetation structure, fuel continuity, and moisture-related landscape conditions requires further research within the Mesoamerican rainforests but could provide insights for designing effective restoration strategies [18]. This knowledge could aid in predicting fire severity based on fuel type, fuel moisture, vegetation structure, and microtopography, thereby supporting the development of localized risk maps and identifying priority areas for intervention. Further integration with information on fuel moisture, vegetation structure, and microtopography could also strengthen the capacity to assess and potentially predict fire severity across larger spatial domains.

Finally, this study provides spatially explicit evidence of fire severity dynamics and post-fire vegetation recovery in a seasonal rainforest invaded by *P. aquilinum*. Several limitations should nevertheless be considered, including the relatively coarse spatial resolution of MODIS data, the site-specific applicability of dNBR thresholds, the use of a single post-fire Sentinel-2 image, limited field sampling, the indirect measurement of fire intensity, and the focus on a single ejido. Future studies should integrate higher-resolution imagery, LiDAR, UAV-based surveys, and long-term field monitoring to refine fire-severity assessments and better characterize vegetation recovery trajectories. The identification

of areas with a higher likelihood of fire occurrence and characterization of potential fire severity provide a basis for quantifying biomass before and after fire events and for directly measuring fire intensity during active burning. Although *P. aquilinum* has been present in the Yucatán Peninsula for a long time, historical changes in land use and agricultural practices have influenced its distribution and its relationship with fire [25,44]. Therefore, a broader understanding of fire ecological processes, as well as historical and contemporary human intervention across the Mesoamerican rainforest is still needed. Recurrent fires in *P. aquilinum*-dominated areas highlight the need for restoration strategies that reduce fuel continuity, promote native regeneration, and disrupt potential fire–bracken feedbacks, thereby strengthening the long-term resilience of these ecosystems.

5. Conclusions

This study provides evidence that seasonal rainforests in the southern Yucatán Peninsula dominated by *P. aquilinum* experience recurrent fire events, with a mean interval of approximately five years between recorded fires. The integration of MODIS and Sentinel-2 imagery, supported by field observations and UAV data, revealed broadly consistent fire-severity patterns between the 2020 and 2024 fire events. Areas dominated by *P. aquilinum* were consistently associated with higher fire severity and limited woody vegetation recovery, whereas areas with greater tree cover were generally associated with lower severity classes. These findings indicate a close association between vegetation composition and fire severity and are consistent with a fire–vegetation feedback that may reinforce recurrent burning and constrain forest regeneration. The results highlight the importance of managing *P. aquilinum* dominance, promoting native tree regeneration, maintaining moisture-retaining vegetation structures, and reducing fuel continuity to enhance ecosystem resilience. Such strategies could help weaken the fire–vegetation feedback and support the long-term conservation and restoration of communal tropical forest landscapes in the southern Mesoamerican rainforest region.

Author Contributions: Conceptualization, J.F.L.-T., J.M.C.-S. and J.C.A.-H.; data curation, J.F.L.-T. and J.M.C.-S., formal analysis, J.F.L.-T., J.M.C.-S. and J.C.A.-H.; funding acquisition, J.F.L.-T. and J.M.C.-S.; investigation, J.F.L.-T., J.M.C.-S., J.C.A.-H. and P.A.M.-M.; methodology, J.F.L.-T. and J.M.C.-S.; project administration, J.F.L.-T. and J.M.C.-S.; resources, J.F.L.-T.; supervision, P.A.M.-M.; validation, J.F.L.-T. and J.M.C.-S.; visualization, J.F.L.-T., J.M.C.-S. and J.C.A.-H.; writing—original draft preparation, J.F.L.-T.; writing—review and editing, J.C.A.-H. and P.A.M.-M. All authors have read and agreed to the published version of the manuscript.

Funding: This research received no external funding.

Institutional Review Board Statement: Not applicable.

Informed Consent Statement: Not applicable.

Data Availability Statement: The burned-area records derived from the Moderate Resolution Imaging Spectroradiometer (MODIS) are publicly available through the Fire Information for Resource Management System (FIRMS) of NASA (https://firms.modaps.eosdis.nasa.gov). Sentinel-2 Level-2A satellite imagery and their B8 and B12 bands, used to calculate the NBR spectral index, are publicly available through the Copernicus platform (https://www.copernicus.eu/). All datasets used in this study are publicly accessible from these sources.

Acknowledgments: The first author gratefully acknowledges the Secretariat of Science, Humanities, Technology and Innovation (SECIHTI) for the doctoral scholarship (number 792367) awarded to support his graduate studies. The authors have reviewed and edited the output and take full responsibility for the content of this publication.

Conflicts of Interest: The authors declare no conflicts of interest.

Abbreviations

The following abbreviations are used in this manuscript:

A	Acahual
BA	Basal Area
BF	Bracken Fern
BG	Bare Ground
DA	Damaged Acahual
DBH	Diameter at breast height
dNBR	Differenced Normalized Burn Ratio
G	Grassland
HS	High Severity
LS	Low Severity
MH	Moderate–High Severity
ML	Moderate–Low Severity
MODIS	Moderate-Resolution Imaging Spectroradiometer
UAV	Unmanned Aerial Vehicle
UB	Unburned
USGS	United States Geological Survey
YA	Young Acahual

References

1. Artés, T.; Oom, D.; de Rigo, D.; Durrant, T.H.; Maianti, P.; Libertà, G.; San-Miguel-Ayanz, J. A Global Wildfire Dataset for the Analysis of Fire Regimes and Fire Behaviour. *Sci. Data* **2019**, *6*, 296. [CrossRef] [PubMed]
2. Tyukavina, A.; Potapov, P.; Hansen, M.C.; Pickens, A.H.; Stehman, S.V.; Turubanova, S.; Parker, D.; Zalles, V.; Lima, A.; Kommareddy, I.; et al. Global Trends of Forest Loss Due to Fire From 2001 to 2019. *Front. Remote Sens.* **2022**, *3*, 825190. [CrossRef]
3. van Wees, D.; van der Werf, G.R.; Randerson, J.T.; Andela, N.; Chen, Y.; Morton, D.C. The Role of Fire in Global Forest Loss Dynamics. *Glob. Change Biol.* **2021**, *27*, 2377–2391. [CrossRef] [PubMed]
4. Amos, C.; Petropoulos, G.P.; Ferentinos, K.P. Determining the Use of Sentinel-2A MSI for Wildfire Burning & Severity Detection. *Int. J. Remote Sens.* **2019**, *40*, 905–930. [CrossRef]
5. Chuvieco, E.; Mouillot, F.; van der Werf, G.R.; San Miguel, J.; Tanase, M.; Koutsias, N.; García, M.; Yebra, M.; Padilla, M.; Gitas, I.; et al. Historical Background and Current Developments for Mapping Burned Area from Satellite Earth Observation. *Remote Sens. Environ.* **2019**, *225*, 45–64. [CrossRef]
6. Juan Baeza, I.B.; Martínez-Garza, C.; Jardel-Peláez, E.J. Efecto de La Severidad de Incendio En La Estructura y Regeneración Del Bosque Tropical de Pino-Implicaciones Para Su Restauración. *Bot. Sci.* **2024**, *102*, 346–368. [CrossRef]
7. Maldonado Méndez, M.L.; Rodríguez Trejo, D.A.; Guízar Nolasco, E.; Velázquez Martínez, J.; Náñez Jiménez, S. Reducción En Riqueza de Especies Arbóreas Por Incendios En La Reserva Selva El Ocote, Chiapas. *Cienc. For. México* **2009**, *34*, 127–148.
8. Warner, T.A.; Skowronski, N.S.; Gallagher, M.R. High Spatial Resolution Burn Severity Mapping of the New Jersey Pine Barrens with WorldView-3 near-Infrared and Shortwave Infrared Imagery. *Int. J. Remote Sens.* **2017**, *38*, 598–616. [CrossRef]
9. White, L.A.; Gibson, R.K. Comparing Fire Extent and Severity Mapping between Sentinel 2 and Landsat 8 Satellite Sensors. *Remote Sens.* **2022**, *14*, 1661. [CrossRef]
10. Keeley, J.E. Fire Intensity, Fire Severity and Burn Severity: A Brief Review and Suggested Usage. *Int. J. Wildland Fire* **2009**, *18*, 116–126. [CrossRef]
11. Key, C.H.; Benson, N.C. *Landscape Assessment (LA): Sampling and Analysis Methods*; General Technical Report RMRS-GTR-164-CD; USDA Forest Service: Washington, DC, USA, 2006; p. 55.
12. Arellano, S.; Vega, J.A.; Rodríguez y Silva, F.; Fernández, C.; Vega-Nieva, D.; Álvarez-González, J.G.; Ruiz-González, A.D. Validación de Los Índices de Teledetección dNBR y RdNBR Para Determinar La Severidad Del Fuego En El Incendio Forestal de Oia-O Rosal (Pontevedra) En 2013. *Rev. Teledetec.* **2017**, *49*, 49–61. [CrossRef]
13. Montorio Lloveria, R.; Pérez-Cabello, F.; García-Martín, A.; Vlassova, L.; De la Riva Fernández, J. La Severidad Del Fuego: Revisión de Conceptos, Métodos y Efectos Ambientales. In *Geoecología, Cambio Ambiental y Paisaje: Homenaje al Profesor José María García-Ruiz*; Arnáez, J., González-Sampériz, P., Lasanta, T., Valero-Garcés, B.L., Eds.; Instituto Pirenaico de Ecología: Zaragoza, Spain, 2014; pp. 427–440.
14. Filipponi, F. BAIS2: Burned Area Index for Sentinel-2. *Proceedings* **2018**, *2*, 364. [CrossRef]

15. Han, A.; Qing, S.; Bao, Y.; Na, L.; Bao, Y.; Liu, X.; Zhang, J.; Wang, C. Short-Term Effects of Fire Severity on Vegetation Based on Sentinel-2 Satellite Data. *Sustainability* **2021**, *13*, 432. [CrossRef]
16. Llorens, R.; Sobrino, J.A.; Fernández, C.; Fernández-Alonso, J.M.; Vega, J.A. A Methodology to Estimate Forest Fires Burned Areas and Burn Severity Degrees Using Sentinel-2 Data. Application to the October 2017 Fires in the Iberian Peninsula. *Int. J. Appl. Earth Obs. Geoinf.* **2021**, *95*, 102243. [CrossRef]
17. Giddey, B.L.; Baard, J.A.; Kraaij, T. Verification of the Differenced Normalised Burn Ratio (dNBR) as an Index of Fire Severity in Afrotemperate Forest. *S. Afr. J. Bot.* **2022**, *146*, 348–353. [CrossRef]
18. dos Santos, S.M.B.; Bento-Gonçalves, A.; Franca-Rocha, W.; Baptista, G. Assessment of Burned Forest Area Severity and Postfire Regrowth in Chapada Diamantina National Park (Bahia, Brazil) Using dNBR and RdNBR Spectral Indices. *Geosciences* **2020**, *10*, 106. [CrossRef]
19. Sandamali, K.U.J.; Chaturanga, K.A.M. Quantification of Burned Severity of the Forest Fire Using Sentinel-2 Remote Sensing Images: A Case Study in the Ella Sri Lanka. *J. Environ. Sci.* **2021**, *3*, 1–12.
20. Sahdev, S. Forest Fire Severity Mapping of Humid Tropical Regions: A Geospatial Perspective. *Int. J. Aquat. Sci.* **2021**, *12*, 1420–1431.
21. Gibson, R.; Danaher, T.; Hehir, W.; Collins, L. A Remote Sensing Approach to Mapping Fire Severity in South-Eastern Australia Using Sentinel 2 and Random Forest. *Remote Sens. Environ.* **2020**, *240*, 111702. [CrossRef]
22. Díaz-Gallegos, J.R.; Mas, J.-F.; Velázquez-Montes, A. Monitoreo de Los Patrones de Deforestación En El Corredor Biológico Mesoamericano, México. *Interciencia* **2008**, *33*, 882–890.
23. Mascorro, V.S.; Coops, N.C.; Kurz, W.A.; Olguín, M. Attributing Changes in Land Cover Using Independent Disturbance Datasets: A Case Study of the Yucatan Peninsula, Mexico. *Reg. Environ. Change* **2016**, *16*, 213–228. [CrossRef]
24. Ramírez-Delgado, J.P.; Christman, Z.; Schmook, B. Deforestation and Fragmentation of Seasonal Tropical Forests in the Southern Yucatán, Mexico (1990–2006). *Geocarto Int.* **2014**, *29*, 822–841. [CrossRef]
25. Ramírez Trejo, M.d.R.; Pérez-García, B.; Pérez-Salicrup, D.R.; Orozco-Segovia, A. Effect of Fire on the Germination of Spores of Pteridium Caudatum, an Invasive Fern. *J. Trop. Ecol.* **2010**, *26*, 457–465. [CrossRef]
26. Suazo-Ortuño, I.; Lopez-Toledo, L.; Alvarado-Díaz, J.; Martínez-Ramos, M. Land-use Change Dynamics, Soil Type and Species Forming Mono-dominant Patches: The Case of *Pteridium aquilinum* in a Neotropical Rain Forest Region. *Biotropica* **2015**, *47*, 18–26. [CrossRef]
27. Jean Baptiste, A.; Macario, P.A.; Islebe, G.A.; Vargas-Larreta, B.; Pool, L.; Valdez-Hernández, M.; López-Martínez, J.O. Secondary Succession under Invasive Species (*Pteridium aquilinum*) Conditions in a Seasonal Dry Tropical Forest in Southeastern Mexico. *PeerJ* **2019**, *7*, e6974. [CrossRef] [PubMed]
28. CONABIO. *Áreas de Importancia Para La Conservación de Las Aves, 2015, Escala: 1:250000*; CONABIO: Mexico City, Mexico, 2015.
29. CONABIO. *Áreas Naturales Protegidas Federales de México*; CONABIO: Mexico City, Mexico, 2023.
30. RAN. *Datos Geográficos Perimetrales de Los Núcleos Agrarios Certificados Por Estado*; RAN: Mexico City, Mexico, 2017.
31. INEGI. *Conjunto de Datos Vectoriales de Información Topográfica E16A54 (Altos de Sevilla) Escala 1:50 000*; Instituto Nacional de Estadística y Geografía: Aguascalientes, Mexico, 2022.
32. INEGI. *Conjunto de Datos Vectoriales de Uso Del Suelo y Vegetación Escala 1:250 000, Serie VII*; INEGI: Aguascalientes, Mexico, 2018.
33. Flores-Garnica, J.G.; Flores-Rodríguez, A.G.; Rivera-Leyva, R.R.; Arellano-Martin, F.; Ursúa-Guerrero, F.E.; Ortiz-Moreno, F.Á.O.; Gutierrez-Carbonell, D. Evaluación Remota de La Recuperación de La Vegetación Afectada Por Incendios Forestales. *e-CUCBA* **2022**, *10*, 213–222. [CrossRef]
34. Pausas, J.G. *Incendios Forestales*; Editorial Catarata y CSIC: Madrid, Spain, 2012; p. 119.
35. Silva-Cardoza, A.I.; Vega-Nieva, D.J.; López-Serrano, P.M.; Corral-Rivas, J.J.; Briseño Reyes, J.; Briones-Herrera, C.I.; Loera Medina, J.C.; Parra Aguirre, E.; Rodríguez-Trejo, D.A.; Jardel-Peláez, E. *Metodología Para La Evaluación de La Severidad de Incendios Forestales En Campo, En Ecosistemas de Bosque Templado de México*; CONAFOR: Guadaljara, Mexico, 2021.
36. Cochrane, M.A. *Tropical Fire Ecology. Climate Change, Land Use and Ecosystem Dynamics*; Springer: Berlin/Heidelberg, Germany, 2009; p. 682.
37. Rodríguez Trejo, D.A. *Incendios de Vegetación—Su Ecología, Manejo e Historia*; Colegio de Postgraduados: Texcoco, Mexico, 2014; p. 891.
38. López-Martínez, J.O.; Sanaphre-Villanueva, L.; Macario-Mendoza, P.A.; Escobar-López, A.; Aragón-Moreno, A.A.; Islebe, G.A.; Vargas-Larreta, B. Identifying Alternative Stable States in a Tropical Landscape Using Remote Sensing. *Plant Ecol.* **2023**, *224*, 605–615. [CrossRef]
39. Hoscilo, A.; Tansey, K.J.; Page, S.E. Post-Fire Vegetation Response as a Proxy to Quantify the Magnitude of Burn Severity in Tropical Peatland. *Int. J. Remote Sens.* **2013**, *34*, 412–433. [CrossRef]
40. Botella-Martínez, M.A.; Fernández-Manso, A. Estudio de La Severidad Post-Incendio En La Comunidad Valenciana Comparando Los Índices dNBR, RdNBR y RBR a Partir de Imágenes Landsat 8. *Rev. Teledetec.* **2017**, *49*, 33–47. [CrossRef]

41. Flores Garnica, J.G.; Flores Rodríguez, A.G.; Rivera Leyva, R.R.; Lomelí Zavala, M.E. Modelos Ecológicos Conceptuales de Selva Baja Subcaducifolia y Selva Mediana Subperennifolia Perturbadas Por Incendios. *e-CUCBA* **2024**, *22*, 34–45. [CrossRef]
42. Peinetti, H.R.; Bestelmeyer, B.T.; Chirino, C.C.; Vivalda, F.L.; Kin, A.G. Thresholds and Alternative States in a Neotropical Dry Forest in Response to Fire Severity. *Ecol. Appl.* **2024**, *34*, e2937. [CrossRef] [PubMed]
43. Trang, P.T.; Andrew, M.E.; Enright, N.J. Burn Severity and Proximity to Undisturbed Forest Drive Post-Fire Recovery in the Tropical Montane Forests of Northern Vietnam. *Fire Ecol.* **2023**, *19*, 47. [CrossRef]
44. Schneider, L.C. Bracken fern invasion in southern Yucatan: A case for land-change science. *Geogr. Rev.* **2004**, *94*, 229–241. [CrossRef]

Disclaimer/Publisher's Note: The statements, opinions and data contained in all publications are solely those of the individual author(s) and contributor(s) and not of MDPI and/or the editor(s). MDPI and/or the editor(s) disclaim responsibility for any injury to people or property resulting from any ideas, methods, instructions or products referred to in the content.